

Exploration of rare earth doped zirconia aerogels for high temperature aerospace applications

Nathaniel Olson¹, Dr. Frances Hurwitz^{2*}, Dr. Jamesa Stokes²,
Dr. Haiquan Guo³, Dr. Jessica Krogstad¹

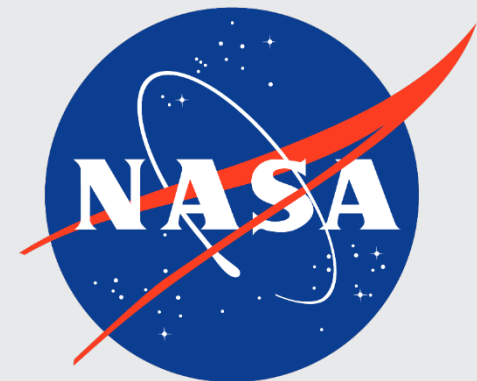
¹University of Illinois at Urbana-Champaign, Department of Materials Science and Engineering, Urbana, IL

²NASA Glenn Research Center, Cleveland, OH

³Universities Space Research Association, Cleveland, OH

* Retired

University of Illinois at Urbana-Champaign
Department of Materials Science & Engineering
Hard Materials Seminar
March 24th, 2022



This work is supported by a NASA Space Technology Research Fellowship

Developing lightweight, high-performance aerospace thermal protection systems (TPS)



TPS Needs:

- Manage heat loads
- Withstand mechanical loads
- Lightweight
- Reusable when possible

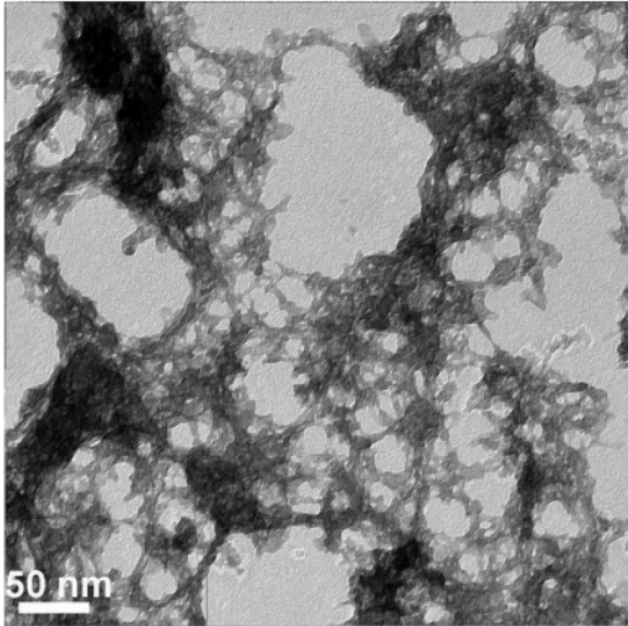


Our Aims:

Reduce **thermal conductivity** to improve performance.

Reduce **mass/volume** to lower costs.

Aerogels are highly insulating and lightweight materials



Highly porous structure of aerogel is responsible for its extremely low thermal conductivity.

Low density = Low solid conductivity

Pore sizes \leq mean free path of gas
= Low gas convection

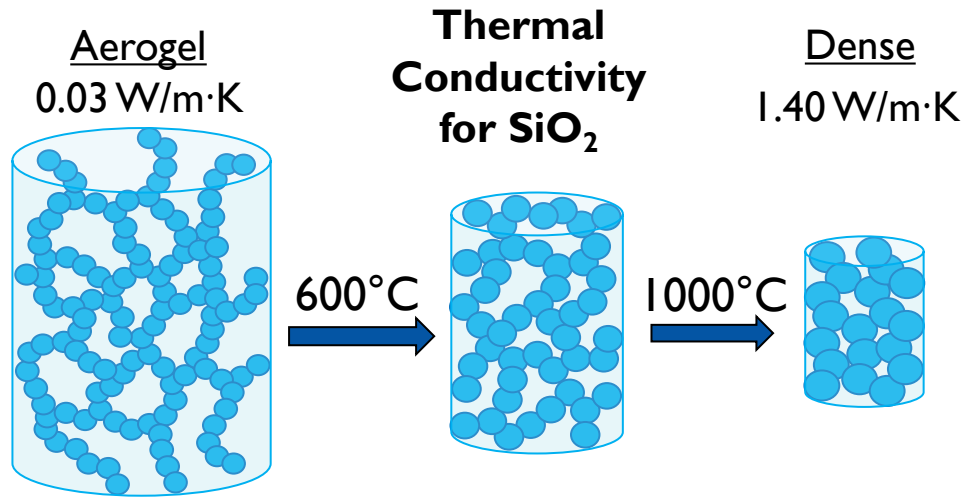
High SSA: 200 to 1000 m²/g

High Porosity: 90 to 99.9%

Low Density: 0.2 to 0.05 g/cm³

Low thermal conductivity:
0.009 W/(m•K) in atmosphere
and 0.003 W/(m•K) under vacuum

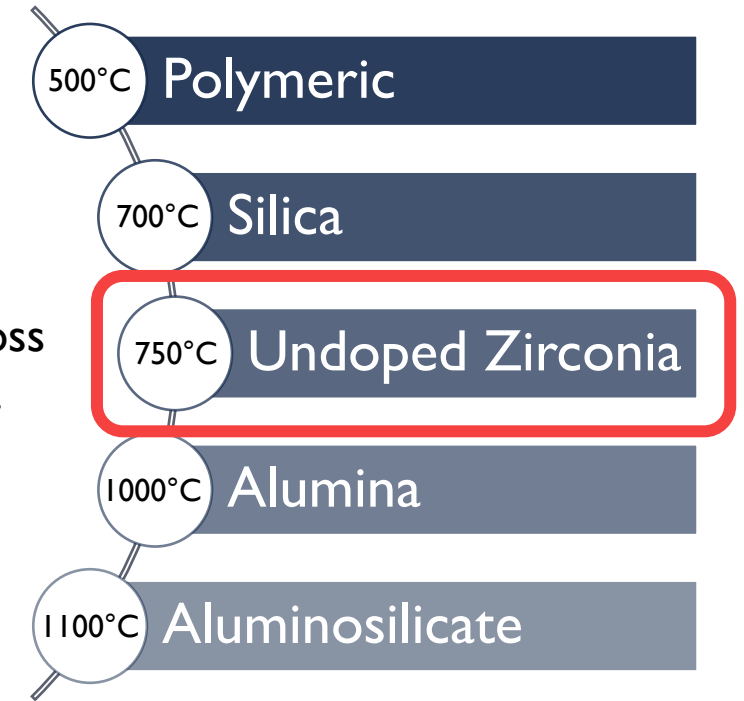
Collapse of pore structure and loss of favorable properties occurs upon thermal exposure



Loss of SSA, porosity
↑ thermal conductivity,
cracking, and shrinkage

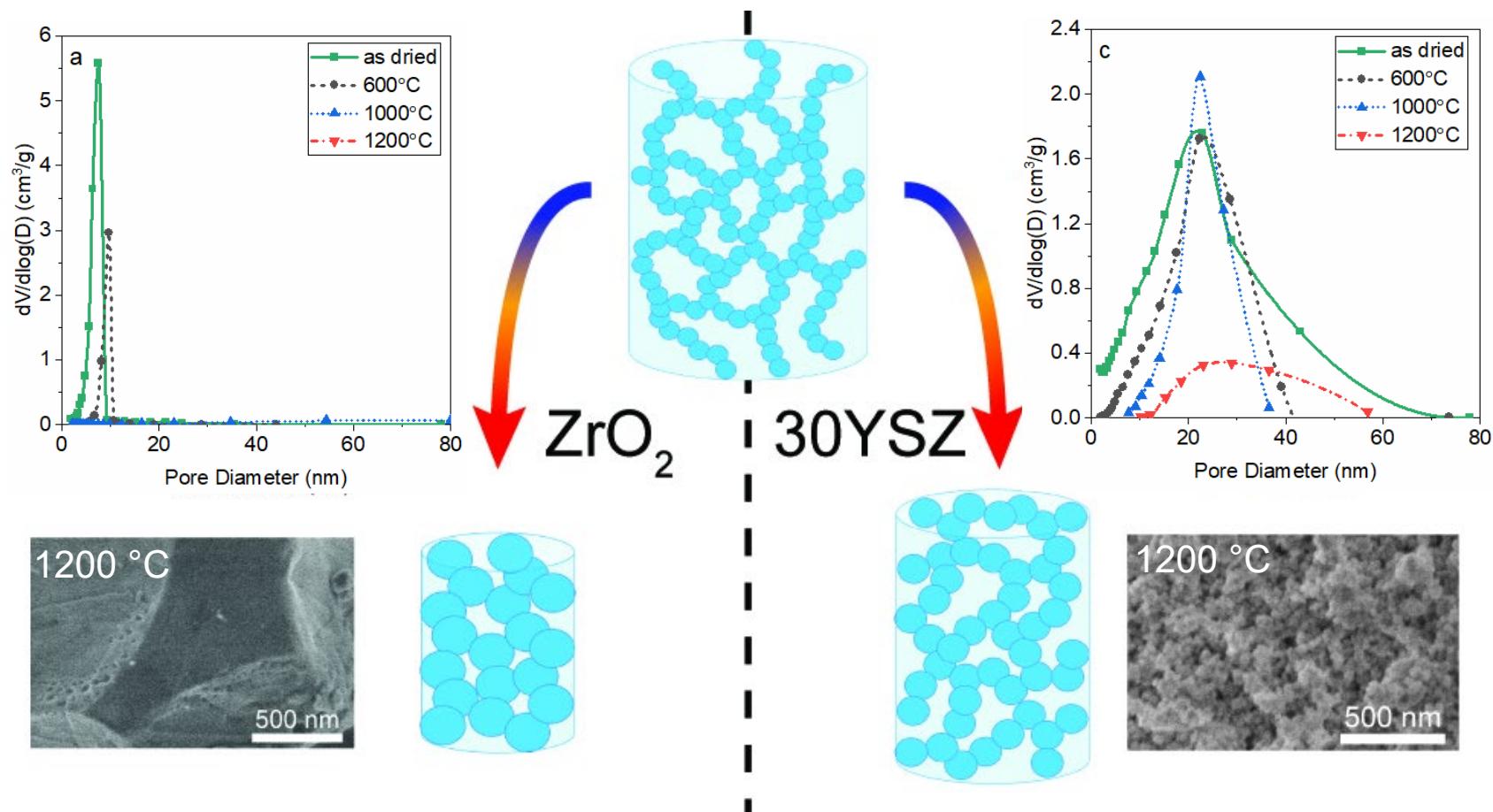
Large SSA & porosity contribute
to driving force for densification

Rapid densification & loss
of porosity beyond...



Develop aerogel to maintain **porosity** at
high temperatures ($\geq 1200^\circ\text{C}$) for use as
insulation in next-gen aerospace applications

High yttria concentration improves thermal stability in yttria-stabilized zirconia (YSZ) aerogels



Doping ZrO₂ with > 30 mol% YO_{1.5} improved the stability of the pore structure to 1200 °C.

Thermodynamics

Lower surface energy with increased yttria content reduces driving force for sintering and densification.

Kinetics

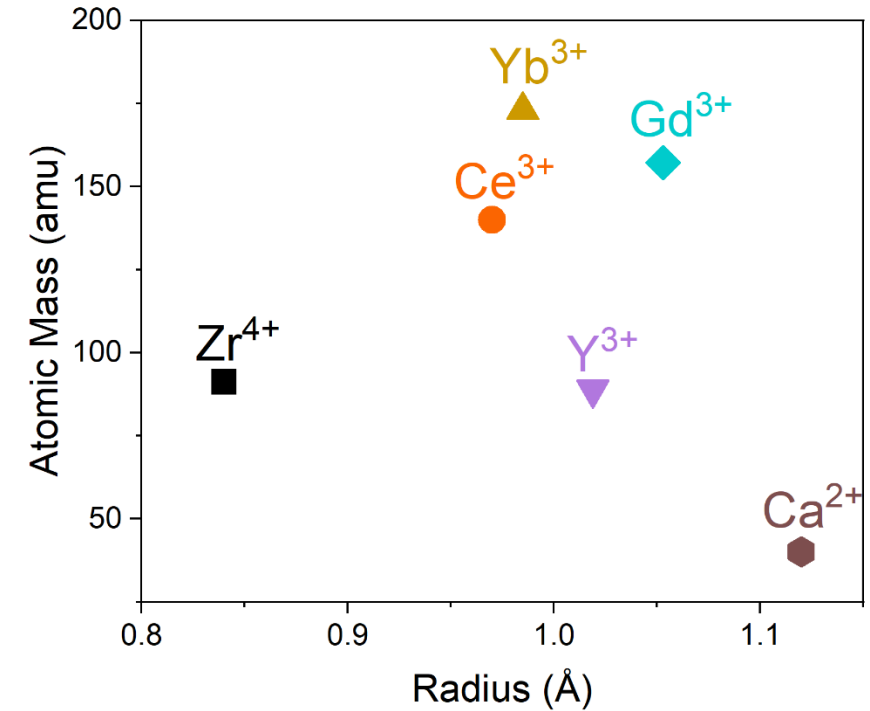
Lower cation diffusivity with increased yttria content reduces rates of sintering and densification.

Study of other dopants (Y, Yb, Gd, Ca, Ce) in zirconia aerogels at 15 and 30 mol% M/(M+Zr)

Further exploration of composition's influence on aerogel thermal stability

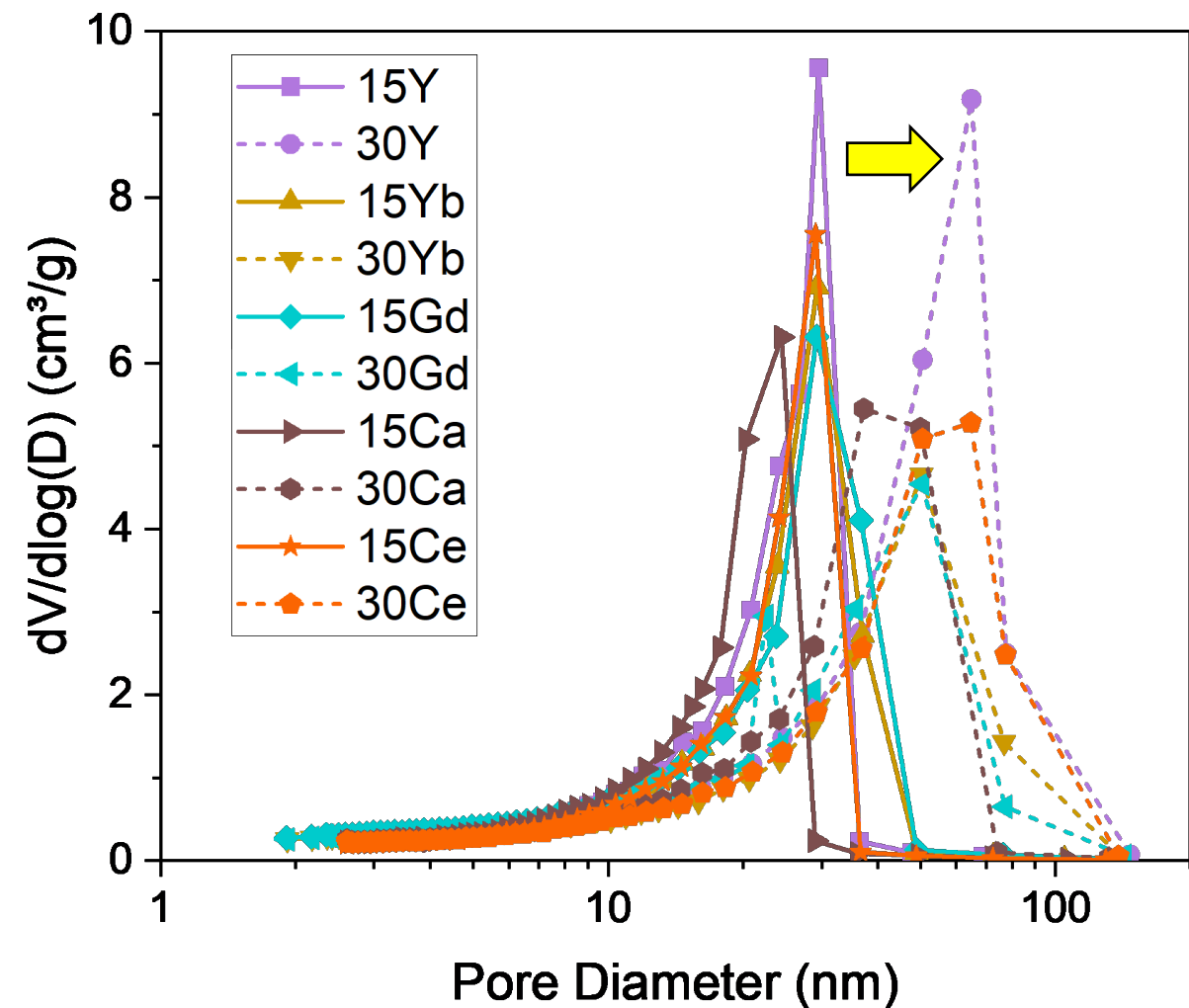
Periodic Table of the Elements

1 IA 1A 1 H Hydrogen 1.008	2 IIA 2A 4 Be Beryllium 9.012																	18 VIIIA 8A 2 He Helium 4.003																	
3 Li Lithium 6.941	11 Na Sodium 22.990	12 Mg Magnesium 24.305	13 B Boron 10.811	14 C Carbon 12.011	15 N Nitrogen 14.007	16 O Oxygen 15.999	17 F Fluorine 18.998	18 Ne Neon 20.180	19 K Potassium 39.098	20 Ca Calcium 40.078	21 Sc Scandium 44.956	22 Ti Titanium 47.867	23 V Vanadium 50.942	24 Cr Chromium 51.996	25 Mn Manganese 54.938	26 Fe Iron 55.845	27 Co Cobalt 58.933	28 Ni Nickel 58.693	29 Cu Copper 63.546	30 Zn Zinc 65.38	31 Ga Gallium 69.723	32 Ge Germanium 72.631	33 As Arsenic 74.922	34 Se Selenium 78.971	35 Br Bromine 79.904	36 Kr Krypton 83.798									
37 Rb Rubidium 85.468	38 Sr Strontium 87.62	39 Y Yttrium 88.906	40 Zr Zirconium 91.224	41 Nb Niobium 92.906	42 Mo Molybdenum 95.95	43 Tc Technetium 98.907	44 Ru Ruthenium 101.07	45 Rh Rhodium 102.906	46 Pd Palladium 106.42	47 Ag Silver 107.868	48 Cd Cadmium 112.414	49 In Indium 114.818	50 Sn Tin 118.711	51 Sb Antimony 121.760	52 Te Tellurium 127.6	53 I Iodine 126.904	54 Xe Xenon 131.294	55 Cs Cesium 132.905	56 Ba Barium 137.328	57-71 Lanthanide Series	72 Hf Hafnium 178.49	73 Ta Tantalum 180.948	74 W Tungsten 183.84	75 Re Rhenium 186.207	76 Os Osmium 190.23	77 Ir Iridium 192.217	78 Pt Platinum 195.085	79 Au Gold 196.967	80 Hg Mercury 200.592	81 Tl Thallium 204.383	82 Pb Lead 207.2	83 Bi Bismuth 208.980	84 Po Polonium [208.982]	85 At Astatine 209.987	86 Rn Radon 222.018
87 Fr Francium 223.020	88 Ra Radium 226.025	89-103 Actinide Series	104 Rf Rutherfordium [261]	105 Db Dubnium [262]	106 Sg Seaborgium [266]	107 Bh Bohrium [264]	108 Hs Hassium [265]	109 Mt Meitnerium [278]	110 Ds Darmstadtium [281]	111 Rg Roentgenium [280]	112 Cn Copernicium [285]	113 Nh Nihonium [286]	114 Fl Flerovium [289]	115 Mc Moscovium [289]	116 Lv Livermorium [293]	117 Ts Tennessine [294]	118 Og Oganesson [294]																		
57 La Lanthanum 138.905	58 Ce Cerium 140.116	59 Pr Praseodymium 140.908	60 Nd Neodymium 144.243	61 Pm Promethium 144.913	62 Sm Samarium 150.36	63 Eu Europium 151.964	64 Gd Gadolinium 157.25	65 Tb Terbium 158.925	66 Dy Dysprosium 162.500	67 Ho Holmium 164.930	68 Er Erbium 167.259	69 Tm Thulium 168.934	70 Yb Ytterbium 173.055	71 Lu Lutetium 174.967																					
89 Ac Actinium 227.028	90 Th Thorium 232.038	91 Pa Protactinium 231.036	92 U Uranium 238.029	93 Np Neptunium 237.048	94 Pu Plutonium 244.064	95 Am Americium 243.061	96 Cm Curium 247.070	97 Bk Berkelium 247.070	98 Cf Californium 251.080	99 Es Einsteinium [254]	100 Fm Fermium 257.095	101 Md Mendelevium 258.1	102 No Nobelium 259.101	103 Lr Lawrencium [262]																					

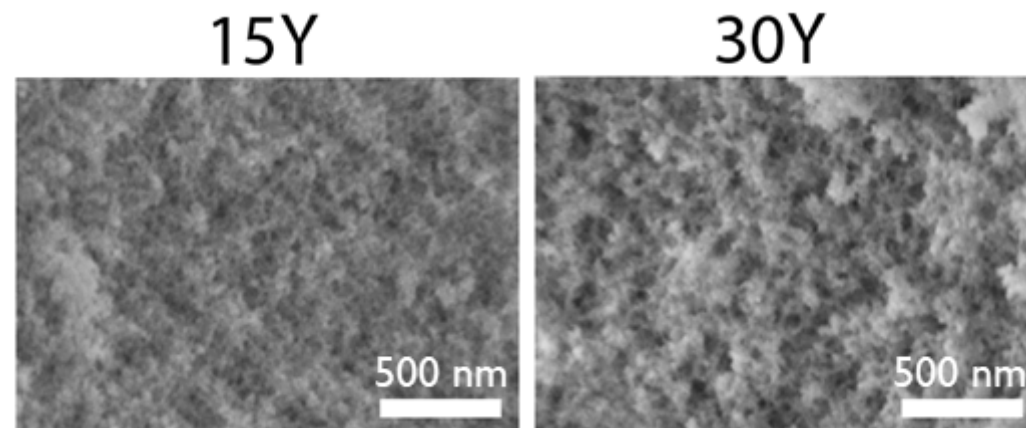


→ Modify thermal conductivity, surface energy and cation diffusivity
 → Connect material properties to changes in structural evolution

As dried structure characterized with nitrogen physisorption and SEM



Increased dopant concentration from 15 to 30 mol% increases average pore size and distribution breadth for *all* dopants.



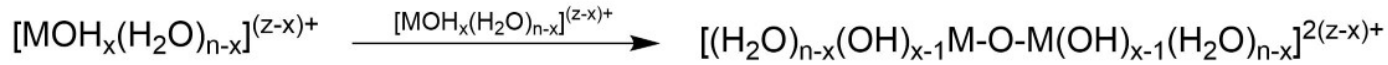
Change in average metal oxidation state hypothesized to increase distribution breadth at 30 mol% dopant

1) Hydrolysis of precursors

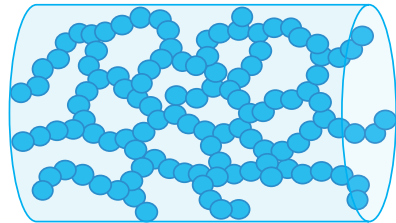


From 15 to 30 mol% dopant we replace more Zr^{4+} with cations of lower charge

2) Condensation and polymerization



... Repeat



Highly porous continuous network

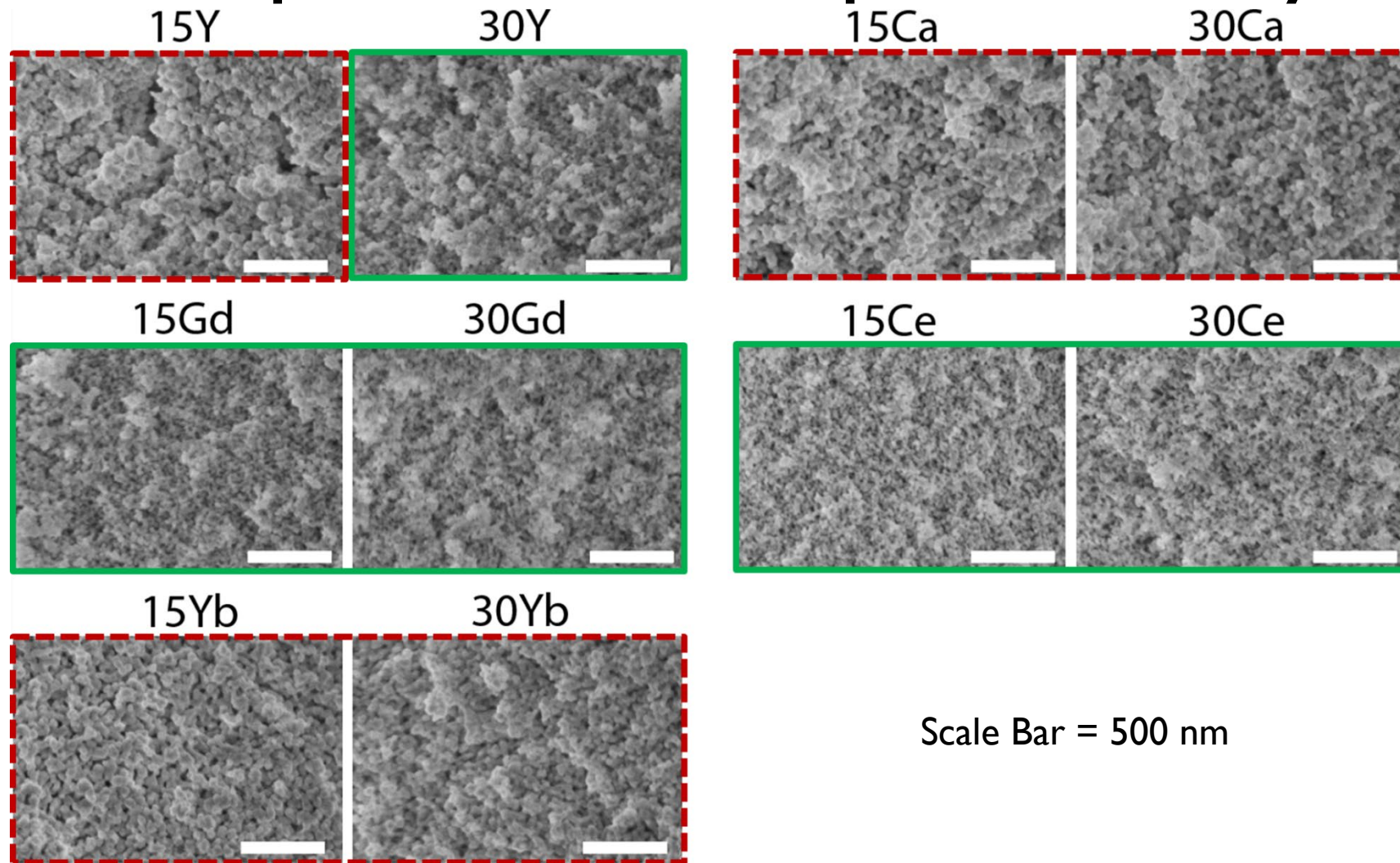
Average metal oxidation state is decreased

Average acidity of $[M(H_2O)_n]^{n+}$ is reduced

Reducing the acidity in turn slows down gel formation. This gives more time for nucleation and growth of particles in the sol.

Larger particles cannot pack as closely together, leading to broader pore size distributions with larger average pore size.

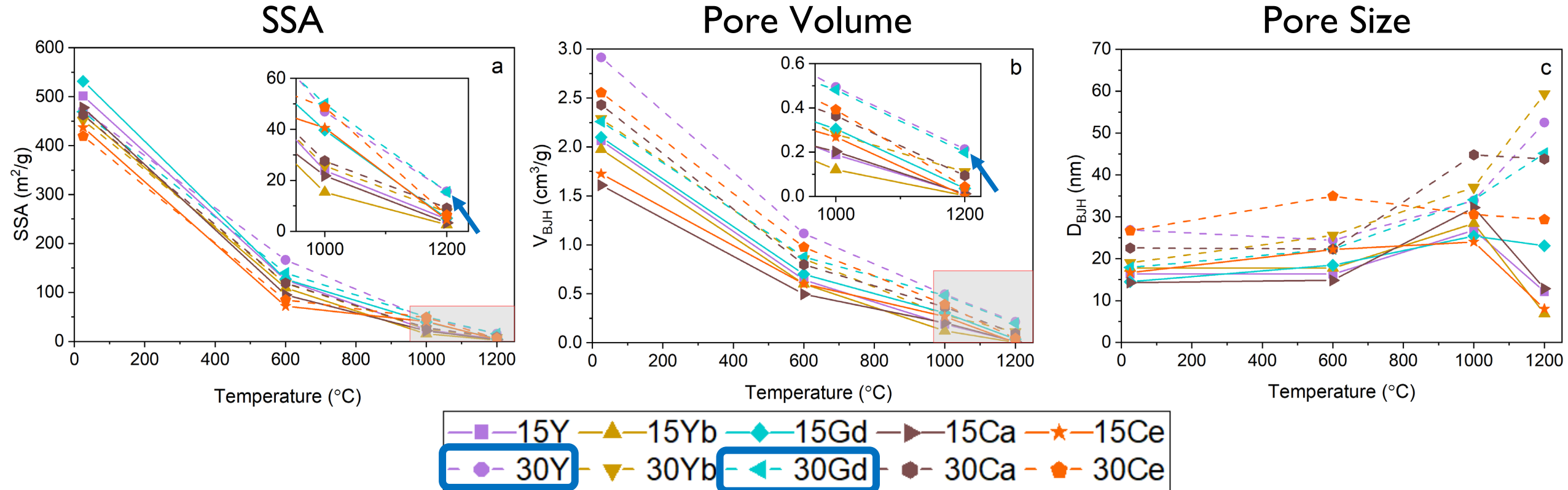
Pore structure stability to 1000 °C appears to be dependent on dopant identity & amount



Red (---): increased particle size and reduction of mesoporosity.
Green (—): porous structure maintained.

Scale Bar = 500 nm

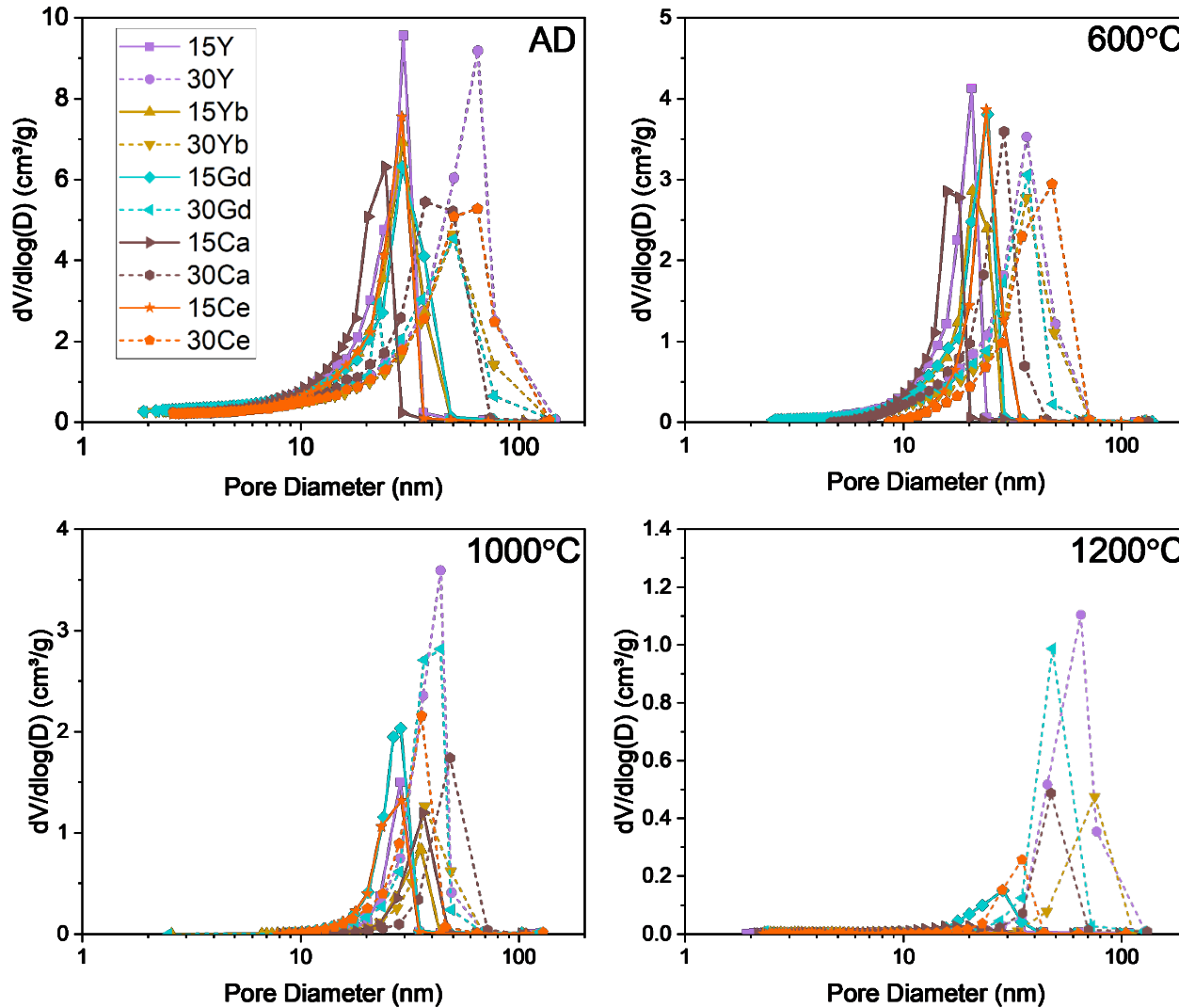
Evaluation of pore structure with nitrogen physisorption quantifies change in performance



Highest Thermal Stability*
 1000 °C: 30Y, 30Gd, 30Ce
 1200 °C: 30Y, 30Gd

In general, 30 mol% dopant maintains higher SSA and pore volume at T ≥ 1000 °C

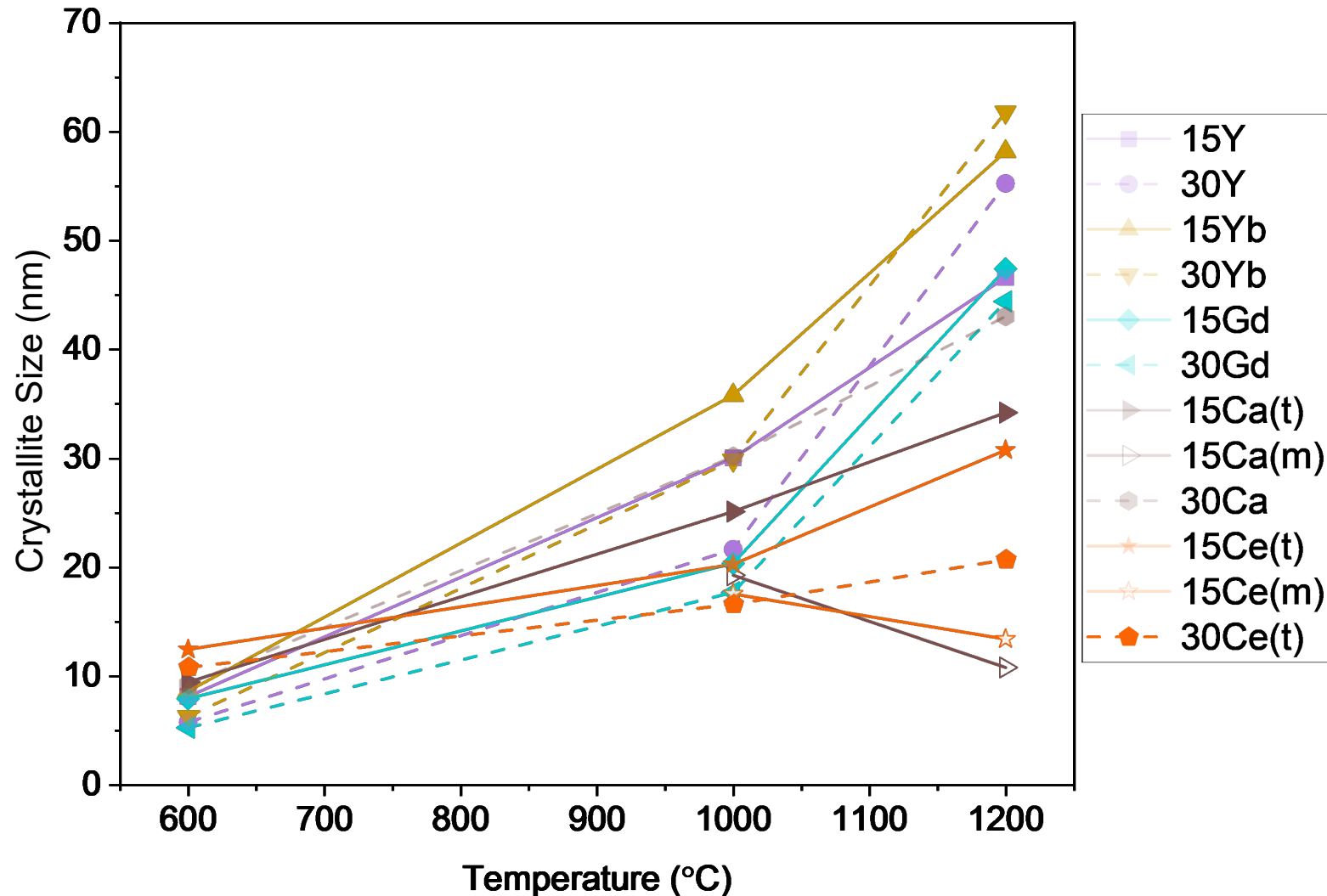
Increased dopant content improves stability of pore structure to 1200 °C



At 600 °C, no visible difference between 15 and 30 mol% MO_x

At 1000 and 1200 °C, it becomes apparent 30 mol% MO_x maintains more porosity. Gd and Y perform the best.

Crystallite growth quantified as a function of dopant identity and concentration

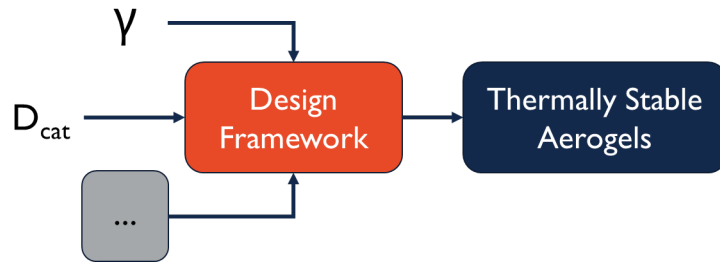


Notable similarity in all trivalent dopants (Y, Yb, Gd) at both 15 and 30 mol%
Gd < Y < Yb

Samples that form mixed tetragonal and monoclinic phases (15Ca, 15Ce) maintain small crystallite size, but have **low phase stability**, which can lead to structure collapse

30Ce maintains a single phase and the smallest crystallite size (by far!) to 1200 °C

Connecting material properties to thermal stability



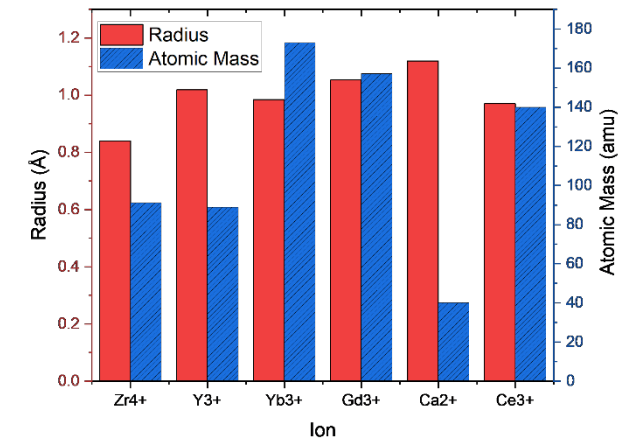
From our work on YSZ, we were able to connect our results to others' measurements of surface energy and cation diffusivity.

But... neither those properties nor others are available for wider ranges of dopants and concentrations

Given this absence, we turned to something readily available: cation properties (mass, radius, charge)

Next, we calculated a weighted average for each material and scaled all properties on [0, 1]

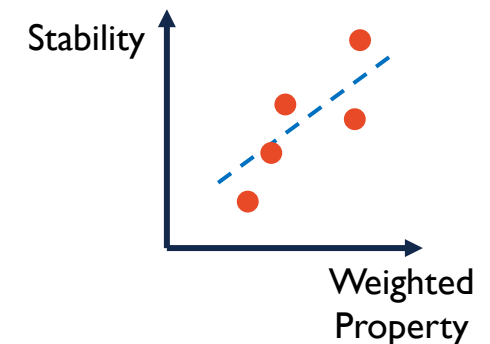
We then performed linear regression on the absolute thermal stability (SSA, V, D, L at a given temperature).



$$\text{Weighted Property} = x_{\text{Zr}} P_{\text{Zr}} + x_{\text{M}} P_{\text{M}}$$

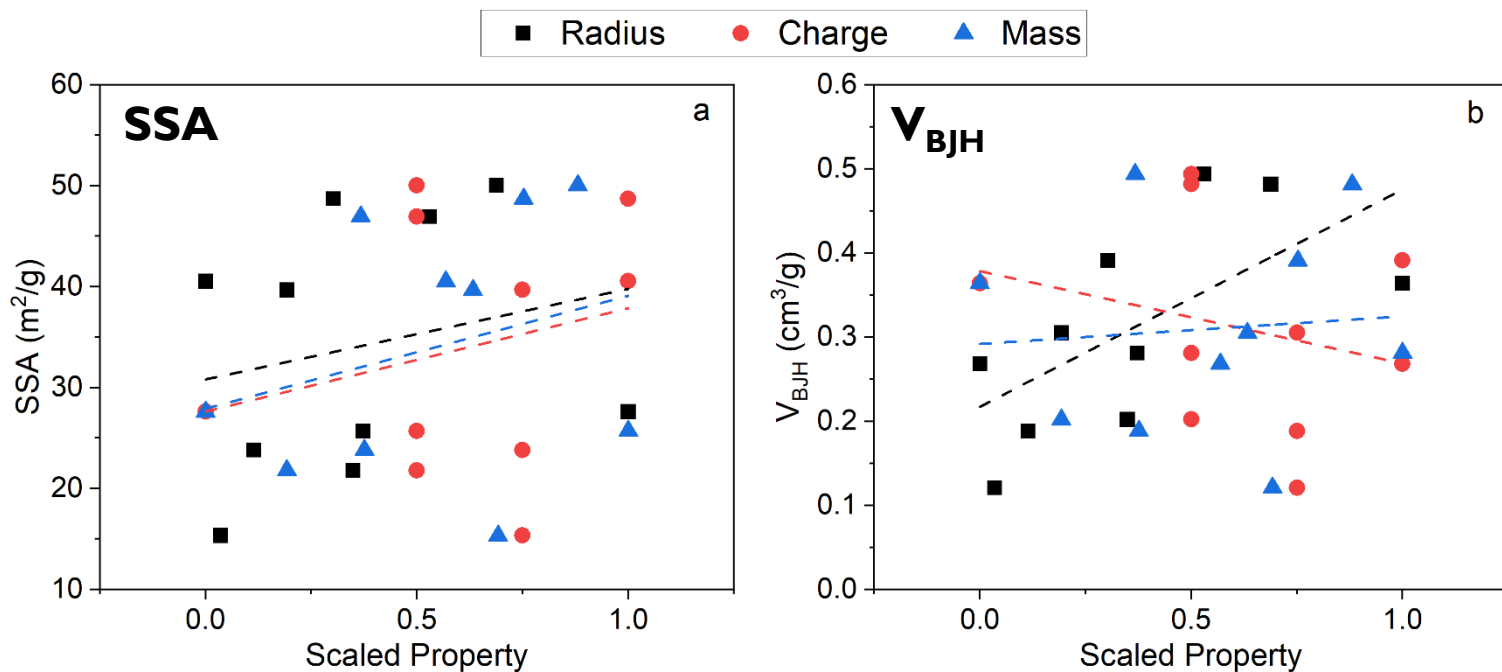
$$x_{\text{M}} = \text{mole fraction } \text{MO}_y$$

$$P_{\text{M}} = \text{property of dopant } \text{M}^{2y+}$$



Currently available properties are insufficient to draw property-stability relationships

How do weighted cation properties relate to **SSA** and **pore volume (V_{BJH})** at **1000 °C**?

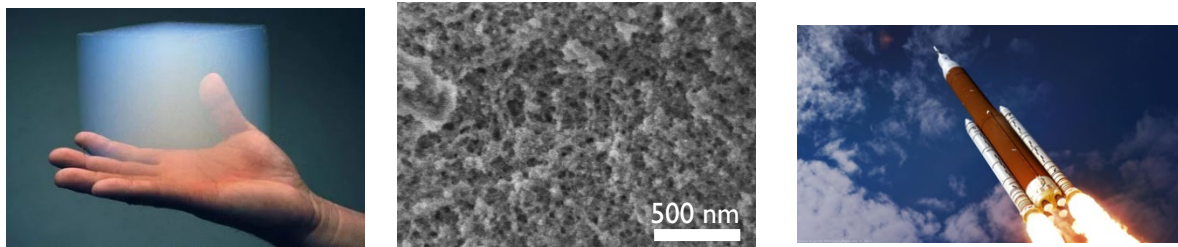


Property	Response at 1000 °C	p-value
Radius	Specific Surface Area (SSA)	0.54
Charge		0.50
Mass		0.44
Radius	Pore Volume (V_{BJH})	0.04
Charge		0.47
Mass		0.8

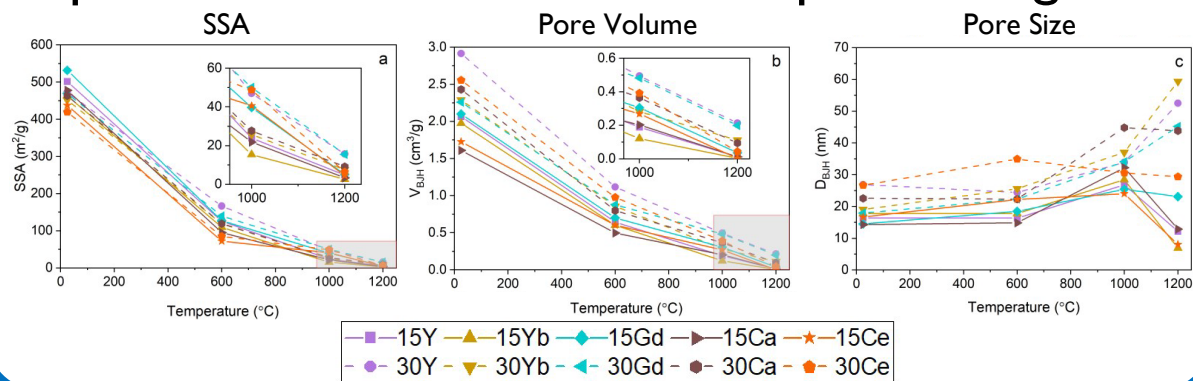
In general, scatter predominates for these relationships and for others not depicted here.

Summary

1. Aerogels are promising candidates for light weight, highly insulating materials, but pore structure must be preserved to $T \geq 1200\text{ }^\circ\text{C}$

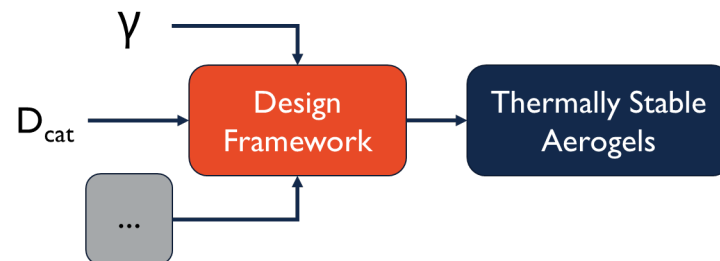


2. Increased dopant concentration from 15 to 30 mol% $M/(M+Zr)$ reduces densification of the pore structure, with Gd and Y performing best.



Looking Forward

1. Wider availability of material property data (surface energy, cation diffusivity, etc.) may help understand source(s) of variability in aerogel thermal stability.



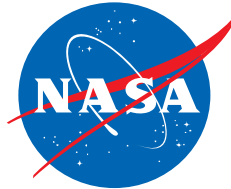
2. Considering the magnitude of improvements achieved by tuning composition, other routes beyond doping may be necessary to achieve thermal stability to temperatures $\geq 1200\text{ }^\circ\text{C}$
3. Evaluation of new synthetic routes to aerogels with dramatically different chemistries and structures that offer improved thermal stability.

Thank you for your attention! Special thanks to...

- Advisor: Dr. Jessica Krogstad (UIUC)
- Technical Collaborator: Dr. Jamesa Stokes (NASA GRC)
- Dr. Frances Hurwitz (NASA GRC, retired)
- Jordan Meyer (UIUC MatSE U-Grad)
- Krogstad Group members
- Others at NASA GRC: Dr. Haiquan (Heidi) Guo, Dr. Richard Rogers, Jessica Cashman

Funding:

- NASA Space Technology Research Fellowship (80NSSC18K1189)



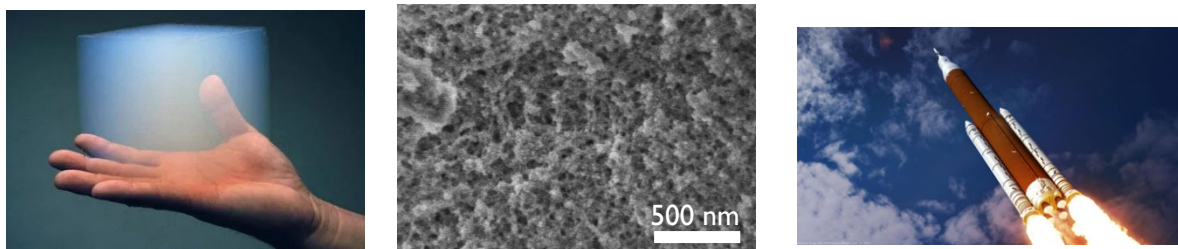
Facilities:

- Materials Research Laboratory, UIUC
- SCS Microanalysis Laboratory, UIUC
- NASA Glenn Research Center

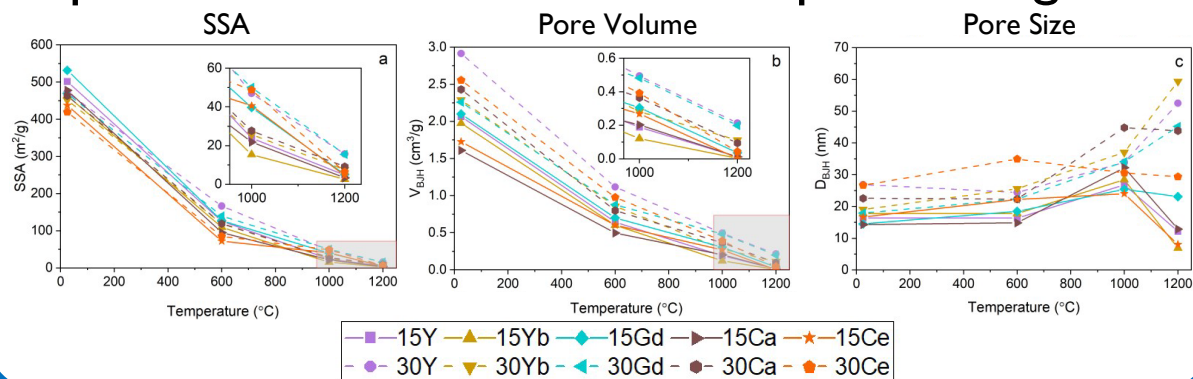


Summary

1. Aerogels are promising candidates for light weight, highly insulating materials, but pore structure must be preserved to $T \geq 1200\text{ }^{\circ}\text{C}$

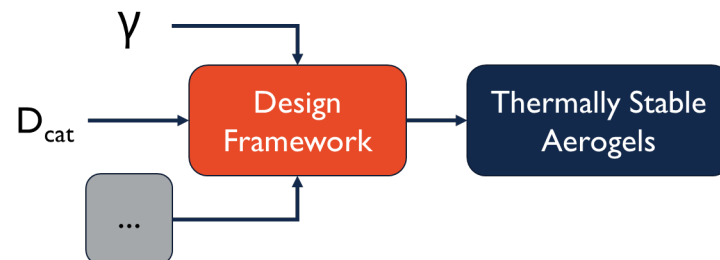


2. Increased dopant concentration from 15 to 30 mol% $M/(M+Zr)$ reduces densification of the pore structure, with Gd and Y performing best.



Looking Forward

1. Wider availability of material property data (surface energy, cation diffusivity, etc.) may help understand source(s) of variability in aerogel thermal stability.



2. Considering the magnitude of improvements achieved by tuning composition, other routes beyond doping may be necessary to achieve thermal stability to temperatures $\geq 1200\text{ }^{\circ}\text{C}$
3. Evaluation of new synthetic routes to aerogels with dramatically different chemistries and structures that offer improved thermal stability.